Sādhanā Vol. 41, No. 5, May 2016, pp. 507–518
DOI 10.1007/s12046-016-0492-9

Statistical feature extraction based iris recognition system

ATUL BANSAL[1,*], RAVINDER AGARWAL[2] and R K SHARMA[3]

[1]Department of Electronics and Communication, G.L.A. University, 17-km stone, NH#2, Delhi-Mathura Road, Mathura 281406, India
[2]Department of Electrical and Instrumentation Engineering, Thapar University, Patiala 147004, India
[3]Department of Computer Science and Engineering, Thapar University, Patiala 147004, India
e-mail: atul.bansal@gla.ac.in

MS received 28 June 2015; revised 17 November 2015; accepted 29 January 2016

Abstract. Iris recognition systems have been proposed by numerous researchers using different feature extraction techniques for accurate and reliable biometric authentication. In this paper, a statistical feature extraction technique based on correlation between adjacent pixels has been proposed and implemented. Hamming distance based metric has been used for matching. Performance of the proposed iris recognition system (IRS) has been measured by recording false acceptance rate (FAR) and false rejection rate (FRR) at different thresholds in the distance metric. System performance has been evaluated by computing statistical features along two directions, namely, radial direction of circular iris region and angular direction extending from pupil to sclera. Experiments have also been conducted to study the effect of number of statistical parameters on FAR and FRR. Results obtained from the experiments based on different set of statistical features of iris images show that there is a significant improvement in equal error rate (EER) when number of statistical parameters for feature extraction is increased from three to six. Further, it has also been found that increasing radial/angular resolution, with normalization in place, improves EER for proposed iris recognition system.

Keywords. Biometric; circular Hough transform; hamming distance, iris recognition system; statistical features.

1. Introduction

Automated security of information and authentication of persons have invariably been an interesting subject of research. Biometric systems for authentication are based on features obtained from one's face [1], finger [2], voice [3] and/or iris [4, 5]. Iris recognition system is widely used in high security areas. A number of researchers have proposed various algorithms for feature extraction. A little work [6, 7] however, has been reported using statistical techniques directly on pixel values in order to extract features. In the subsequent subsections, three phases of IRS, preprocessing, feature extraction and matching are discussed in brief.

1.1 *Image preprocessing*

Preprocessing refers to convert the image of eye into a form from which the desired features can be extracted and used for identification of an individual. Image preprocessing is divided into three steps – iris localization, iris normalization and image enhancement. Iris localization means to detect the inner and outer boundaries of iris, to find and remove the eyelashes of eyelids that might have covered the iris region. Iris normalization is performed to convert the iris image from Cartesian coordinates to polar coordinates. Normalized iris image is a rectangular image with angular and radial resolutions. Normalization helps in removing the dimensional inconsistencies that arise due to variation in illumination, camera distance, angle, etc. while capturing the image of an eye. Now, the obtained normalized image is enhanced to compensate for the low contrast, poor light source and position of light source. A number of algorithms for pre-processing have been proposed and implemented by different researchers [4, 8–11].

1.2 *Feature extraction*

Feature extraction is the next important step after preprocessing. The normalized image is used to extract significant features from iris image by applying suitable transformations. These features are further encoded to make the comparisons between templates more effective. Different techniques like wavelet transform [12], Hilbert transform [13] and Gabor filters [4, 14, 15] are employed on the

*For correspondence

normalized iris image to extract the features from the iris by creating template. Recently, other advanced techniques such as gray level co-occurrence matrix (GLCM) based Harlick features [16], local binary pattern (LBP) [17], triplet half-band filter bank (THFB) [18], and dynamic features (DF) [19], have also been used in iris recognition. Daugman [4] extracted features from iris image by passing it through a bank of Gabor filters and then encoded this phase information to create feature vector. Bodade and Talbar [12] obtained iris features by computing energies and standard deviation of detailed coefficients in 12 directions per stage, at three levels of decomposition. Tisse *et al* [13] used the concept of "analytic image" (2-D Hilbert transform) to extract pertinent information from iris texture. Sundaram and Dhara [16] processed the normalized image by 2-D Haar wavelet and computed GLCM based Haralick features from the low frequency data. He *et al* [17] generated iris feature code by implementing chunked encoding method based on statistical information from an iris's LBP image. Rahulkar and Holambe [18] designed a triplet 2-D bi-orthogonal wavelet basis for iris feature extraction. Costa and Gonzaga [19] extracted Dynamic features from iris image. Their methodology-extracted information about the ways the human eye reacts to light, and used this information for biometric recognition purposes. Ko *et al* [6] used mean of pixel values for extracting features from iris image. They divided the normalized iris image into cells of $m \times n$ pixels size and then created groups consisting of five cells in horizontal and five cells in vertical directions. Mean of pixel values in a cell represented each cell. They first calculated average of means for each group and then calculated cumulative sum for each group by adding the difference between current value and the mean to previous sum starting from cell-1 to cell-5 in a group. After these calculations, iris code is generated for each cell by observing change in cumulative sum. Kyaw [7] utilized statistical feature extraction technique on the iris image without implementing normalization process. He proposed a statistical technique to extract features from segmented image by considering virtual circles on iris image. A difficulty with his technique is that the image is not normalized and thus the system may not work well when there is an inconsistency in the size of the iris due to varying illumination, varying image distance, etc. There is a need to normalize the iris image for more efficient recognition. In this paper, statistical features, namely, mean, median, standard deviation, skewness, kurtosis and coefficient of variation have been extracted from normalized iris image in angular/radial direction.

1.3 *Matching*

Recognition process is carried out using template matching. In template matching, user iris template is compared with the templates from the database using matching metric. The matching metric gives different range of values when a given iris template is compared with the other stored templates. Based upon these range of values, a decision is taken about the identity of a person, i.e., the person is who they claim to be?

2. Preprocessing

Image preprocessing is the preliminary stage of iris recognition system. The purpose of preprocessing is to isolate the iris region from an eye image. In this step, noise in the iris region due to reflection, illumination and occlusion because of eyelids or eyelashes is also minimized. Different researchers have proposed a good number of algorithms for three stages of preprocessing: iris localization, iris normalization and iris image enhancement. Daugman [4] proposed an effective integro-differential operator for detecting inner and outer boundaries of an iris. Tisse *et al* [13], Ballard [20], Wildes *et al* [21], Kong and Zhang [22] and Ma *et al* [23] employed Circular Hough Transform (CHT) for this operation. In this work, segmentation of iris images has been carried out using CHT.

Once iris region is successfully segmented from an eye image, next step is to transform the iris region to the fixed dimensions. The constant dimension of iris region is vital to eliminate the noise due to pupil dilation. Daugman [4] proposed homogeneous rubber sheet model for normalization. This model maps each point within the iris region from Cartesian coordinates to polar coordinates. With centre of the pupil as reference, radial vectors are drawn along the iris region. From the iris region, normalization produces a 2-D array with horizontal dimensions of angular resolution and vertical dimensions of radial resolution as shown in figure 1. Radial resolution represents the number of data points selected along each radial vector and angular resolution represents the number of radial vectors going around the iris region.

Figure 1. Daugman's rubber sheet model.

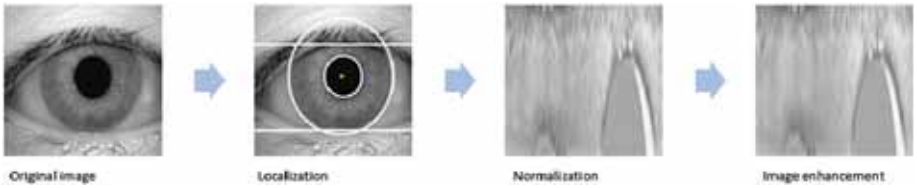

Figure 2. Image preprocessing.

The combinations of radial and angular resolutions considered in the present work are (50, 1000), (100, 1000), (150, 1000) and (200, 1000) while experimenting with radial resolution and (200, 250), (200, 500), (200, 750) and (200, 1000) while experimenting with angular resolution.

The normalized image is enhanced for adjusting the lighting conditions. Local histogram analysis [24] and simple threshold operation [25] have been utilized to reduce the reflection noise. The process of iris image preprocessing is illustrated in figure 2.

3. Feature extraction

In this paper, once a normalized iris image is obtained after preprocessing of an eye image statistical approach has been used for feature extraction. A set of virtual concentric circles is drawn along the iris region as shown in figure 3(a). In figure 3(b), normalized iris image is shown where each row of 2-D array of normalized iris image is equivalent to a virtual circle drawn on the iris region. The features of an iris can be extracted along the concentric circles as well as along the angular direction in the iris region. These statistical features are mean, median, standard deviation, skewness, kurtosis, and co-efficient of variation.

In this paper, two sets of experiments have been conducted. In the first experiment, statistical features have been computed along each row of 2-D normalized array. While in second experiment, statistical features have been calculated along each column of 2-D normalized array. Here, the effect of number of statistical features as well as radial and angular resolutions while normalization on the performance of proposed IRS has also been analyzed. For both experiments, three parameters, namely, mean, median and standard deviation have initially been used. Next, the system performance has been computed using six parameters, namely, mean, median, standard deviation, skewness, kurtosis and co-efficient of variation. At the same time, effect of radial resolution and effect of angular resolution have also been studied.

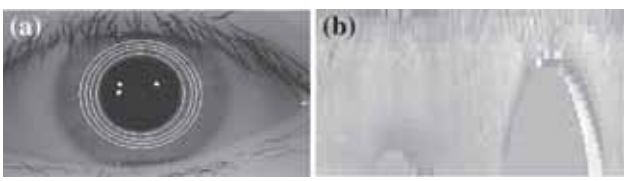

Figure 3. (**a**) Iris image with virtual circles. (**b**) Normalized iris image.

In first experiment, statistical features are computed along each row. The computation gives a set of feature vectors (F_r) for an image. This set is stored in the database for identification process. This set is denoted as

$$F_r = \left(\overline{X}^r, Md^r, s^r, S_k^r, ku^r, CV^r\right), \quad r = 1, 2, 3, \ldots, R \quad (1)$$

where R is the number of rows in normalized iris image, $\overline{X}^r$ is mean of the rth row, Md^r is median of the rth row, s^r is standard deviation of the rth row, S_k^r is skewness of the rth row, ku^r is kurtosis of the rth row, and CV^r is co-efficient of viation of the rth row.

In second experiment, statistical features are computed along each column. This computation gives a set of feature vectors (F_c) for an image. This set is stored in the database for identification process. This set is denoted as

$$F_c = \left(\overline{X}^c, Md^c, s^c, S_k^c, ku^c, CV^c\right), \quad c = 1, 2, 3, \ldots, C \quad (2)$$

where C is the number of columns in normalized iris image, $\bar{X}^c$ is mean of the cth column, Md^c is median of the cth column, s^c is standard deviation of the cth column, S_k^c is skewness of the cth column, ku^c is kurtosis of the cth column, and CV^c is co-efficient of variation of the cth column.

4. Materials and methods

In this work, experiments have been conducted on two databases, namely, "IIT Delhi Iris Database version 1.0" (http://www4.comp.polyu.edu.hk/~csajaykr/IITD/Database_Iris.htm) consisting of 2240 iris images acquired from 224 subjects and interval subset of "CASIA-Iris-V4" (http://www.cbsr.ia.ac.cn/china/Iris_Databases_CH.asp) consisting of 2639 iris images acquired from 249 subjects. Preprocessing, feature extraction and recognition processes have been implemented on these images using image processing module of Matlab 7.1 on Intel Core2 Duo 1.80 GHz processor with 1 GB RAM. In preprocessing, segmentation is carried out using circular Hough transform whereas linear Hough transform has been employed to segment eyelids and a simple thresholding technique for removing eyelashes. Table 1 shows the number of iris images segmented successfully for both the databases.

Table 1. Successfully segmented images.

Database	Number of images considered	Number of images segmented successfully	Result (%)
IITD	2240	2192	97.86
CASIA	2639	2589	98.11

The results in this table are based on visual inspection by authors. The proposed system has been tested only on the successfully segmented iris images.

Further, Daugman's rubber sheet model for normalization and local histogram analysis method for image enhancement have been implemented in this work. Statistical feature extraction technique based on correlation between adjacent pixels has been proposed and implemented.

A pattern matching technique has been used for iris recognition that uses features extracted in the form of F_r or F_c. In this work, similarity of two iris codes is obtained using Hamming distance [4, 6, 7]. Hamming distance requires feature vectors to be converted into binary format. The binary vector in the first experiment is formed by taking the difference between features of the adjacent rows and then thresholding the difference to a binary number whereas, the binary vector in the second experiment is formed by taking the difference between features of the adjacent columns and then thresholding the difference to a binary number. In both experiments, there is a need of 1-bit per feature for truncation. Although, segmentation of eyelids and removal of eyelashes have been considered in this work, rotational noise has not been removed. As such, shifting of templates has not been considered in this study. Hamming distance measures the number of dissimilar bits between two binary vectors and this distance is zero when two vectors are from same iris image. A distance metric of Hamming distance between binary vectors of test image and iris templates stored in the database is generated. Now, minimum of the distance metric is compared with a matching threshold to decide the user as authentic or imposter. Performance of proposed IRS has been measured by recording false acceptance rate (FAR) and false rejection rate (FRR) at different matching thresholds in the distance metric. If the selected minimum Hamming distance is less than matching threshold, the two templates are from same iris image and if it is larger than matching threshold, the subject is considered as an imposter.

5. Results

In this work, two experiments have been conducted that are based on the directions in which statistical features are computed. As stated earlier, these directions are radial direction and angular direction. Performance measurement has been carried out by recording false acceptance rate (FAR) and false rejection rate (FRR) at different matching thresholds for Hamming distance.

5.1 *Feature extraction along concentric circles*

In this experiment, features have been extracted along each row. Number of rows in the normalized image represents radial resolution in normalization process that corresponds to length of one feature. Feature vector as discussed earlier is formed by combining different features.

5.1a *Experimentation with three statistical parameters*: IRS performance has initially been measured by considering three statistical parameters, namely, mean, median and standard deviation. Experiment has been conducted on two different sets of iris databases: IITD iris database version-1.0 and CASIA-Iris-V4 database. FAR and FRR have been computed for 50, 100, 150 and 200 rows in 2-D normalized iris image for the iris images in these databases. Length of feature vector for each feature is therefore 50-bit, 100-bit, 150-bit and 200-bit. Figures 4 and 5 show variations in FAR, FRR for feature vector with different sizes for IITD database and figures 6 and 7 show variations in FAR, and FRR for feature vector with different sizes for CASIA database.

Figures 8 and 9 depict DET curves for IITD and CASIA databases, respectively.

5.1b *Experimentation with six statistical parameters*: IRS performance has been measured by considering six statistical parameters, namely, mean, median, standard deviation, skewness, kurtosis and coefficient of variation in this experiment. Performance of the system has again been tested on the two iris databases: IITD iris database version-1.0 and CASIA-Iris-V4 database. FAR and FRR have been computed for 50, 100, 150 and 200 rows in 2-D normalized iris image. Length of feature vector for each feature is therefore 50-bit, 100-bit, 150-bit and 200-bit. Figures 10 and 11 show variations in FAR and FRR for feature vectors with different sizes for IITD database. Figures 12 and 13 show variations in FAR and FRR for feature vectors with different sizes for CASIA database.

Figures 14 and 15 show DET curves for IITD and CASIA databases, respectively.

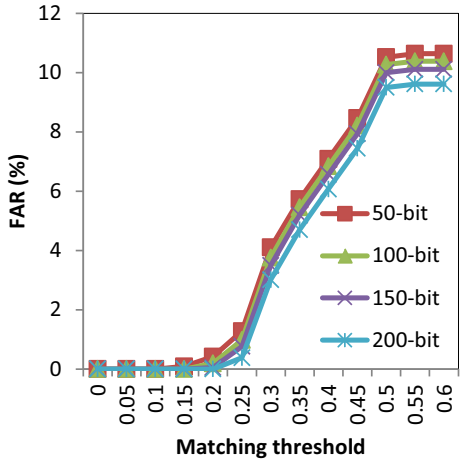

Figure 4. Variation in FAR for different length feature vector for IITD database.

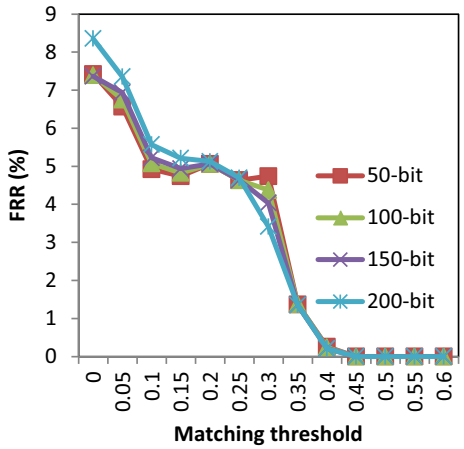

Figure 5. Variation in FRR for different length feature vector for IITD database.

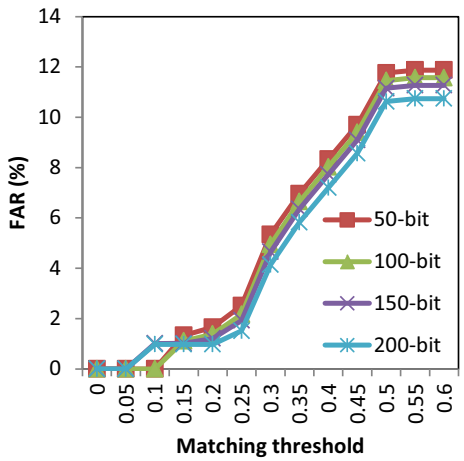

Figure 6. Variation in FAR for different length feature vector for CASIA database.

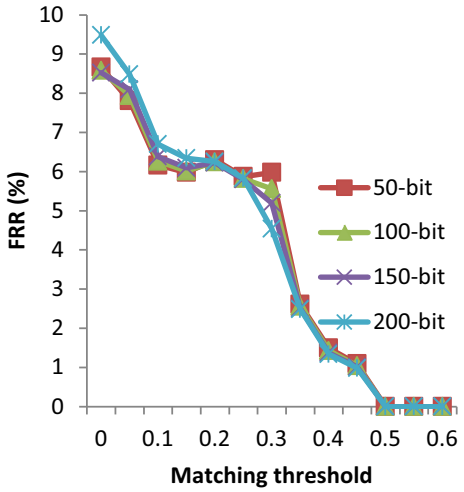

Figure 7. Variation in FRR for different length feature vector for CASIA database.

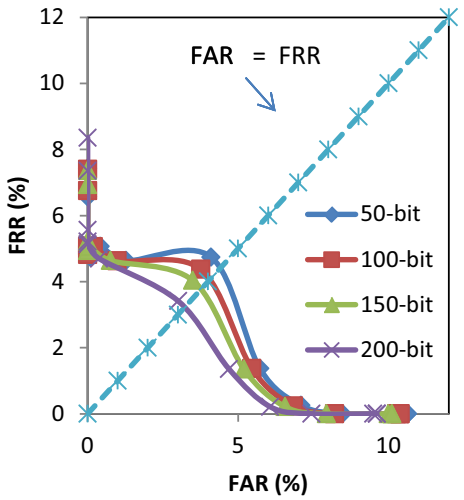

Figure 8. DET curve for different length feature vector for IITD database.

5.2 *Feature extraction along angular direction*

In second experiment, statistical features have been computed along the radial vectors drawn in the iris region extending from pupil–iris boundary to iris–sclera boundary. In 2-D normalized iris image, each column of normalized image corresponds to a radial vector drawn on iris region. Here, features have been extracted along each column of the normalized iris image. Number of columns in the normalized image represents angular resolution in normalization process that corresponds to length of one feature. Feature vector as discussed earlier is calculated by combining different features.

5.2a *Experimentation with three parameters*: IRS performance has been measured by considering three statistical

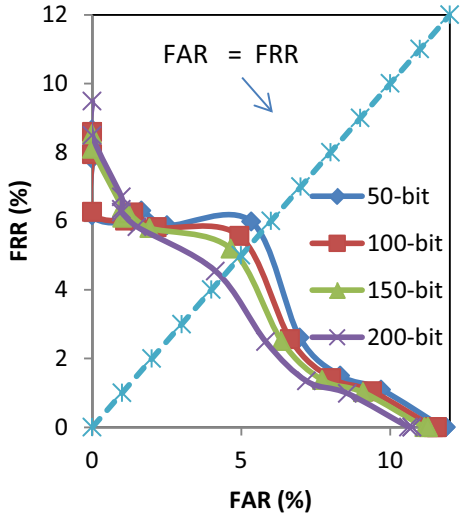

Figure 9. DET curve for different length feature vector for CASIA database.

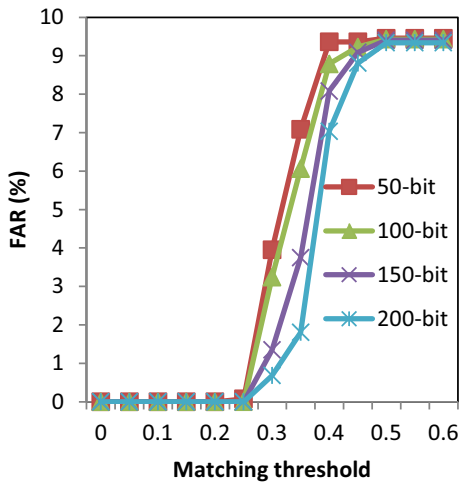

Figure 10. Variation in FAR for different length feature vector for IITD database.

parameters, namely, mean, median and standard deviation in this experiment on the lines similar to feature extraction along radial direction. Experiment has again been conducted on two different sets of iris databases. FAR and FRR have been computed for 250, 500, 750 and 1000 columns in 2-D normalized iris image. Length of feature vector for each feature is thus 250-bit, 500-bit, 750-bit and 1000-bit. Figures 16 and 17 show variations in FAR and FRR for feature vector with different sizes for IITD database and figures 18 and 19 show variations in FAR and FRR for feature vector with different sizes for CASIA database.

Figures 20 and 21 show DET curves for IITD and CASIA databases, respectively. One can infer from these DET curves that EER decreases when feature vector size is increased for both databases.

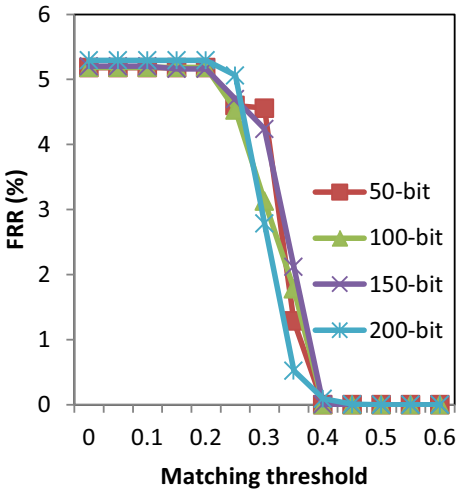

Figure 11. Variation in FRR for different length feature vector for IITD database.

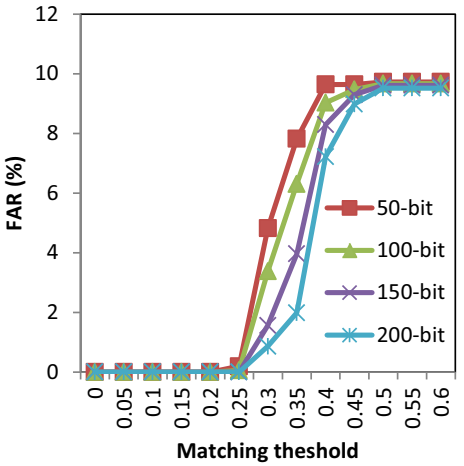

Figure 12. Variation in FAR for different length feature vector for CASIA database.

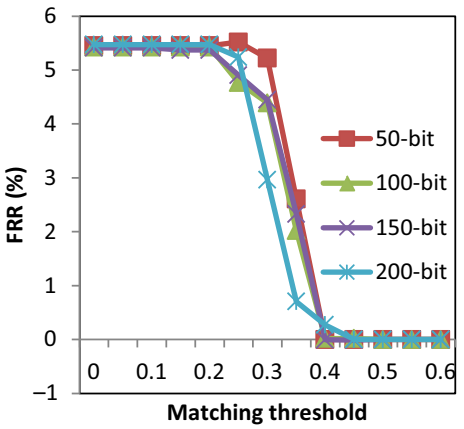

Figure 13. Variation in FRR for different length feature vector for CASIA database.

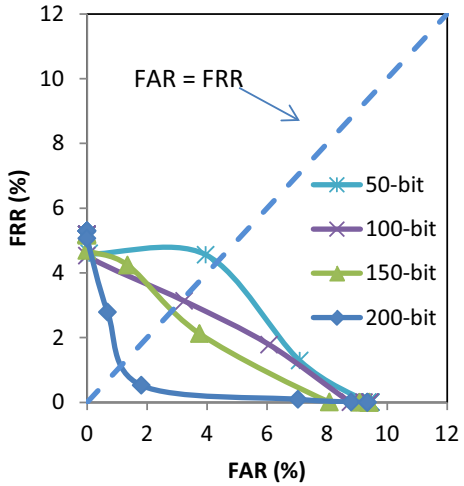

Figure 14. DET curve for different length feature vector for IITD database.

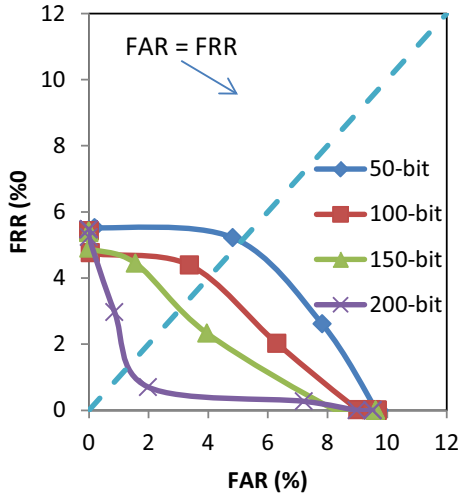

Figure 15. DET curve for different length feature vector for CASIA database.

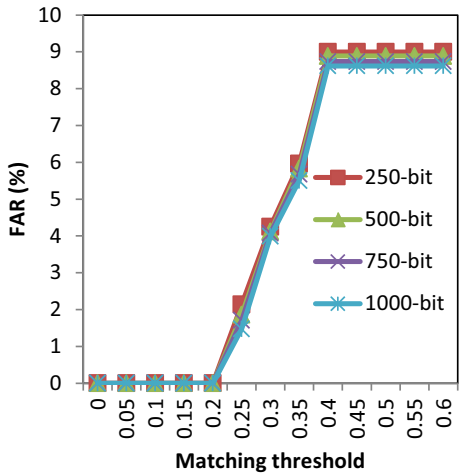

Figure 16. Variation in FAR for different length feature vector for IITD database.

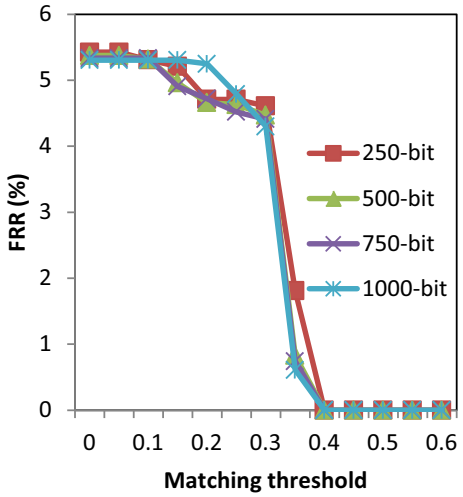

Figure 17. Variation in FRR for different length feature vector for IITD database.

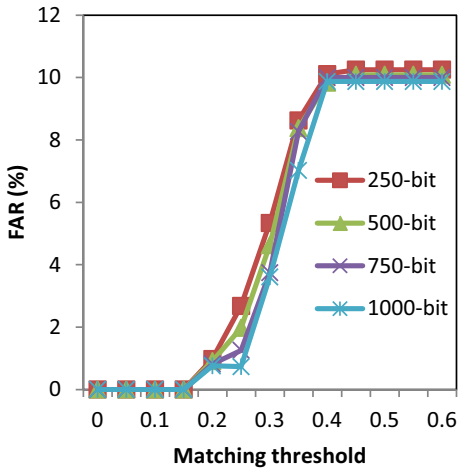

Figure 18. Variation in FAR for different length feature vector for CASIA database.

5.2b *Experimentation with six statistical parameters*: IRS performance is next measured by considering six statistical parameters, namely, mean, median, standard deviation, skewness, kurtosis and coefficient of variation for both databases. FAR and FRR have again been computed for 250, 500, 750 and 1000 columns in 2-D normalized iris image. Figures 22 and 23 show variations in FAR and FRR for feature vector with different sizes for IIT Delhi database and figures 24 and 25 show variations in FAR and FRR for feature vector with different sizes for CASIA database.

6. Discussion

In the first set of experiments, that is feature extraction along concentric circles while considering three parameters one can note from figures 4, 5, 6 and 7 that increase in the

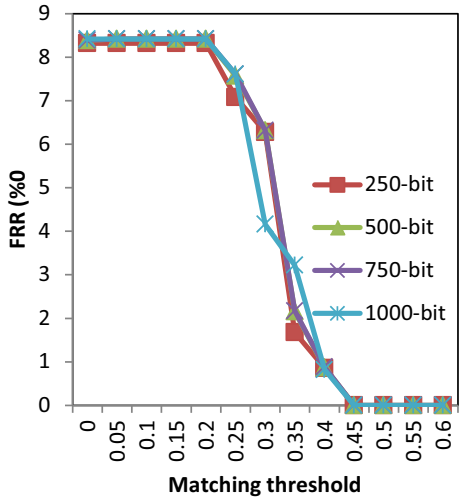

Figure 19. Variation in FRR for different length feature vector for CASIA database.

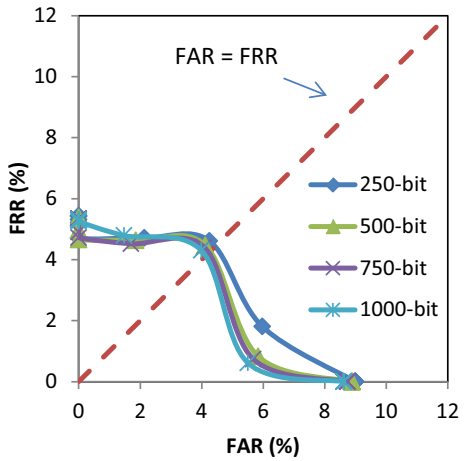

Figure 20. DET curve for different length feature vector for IITD database.

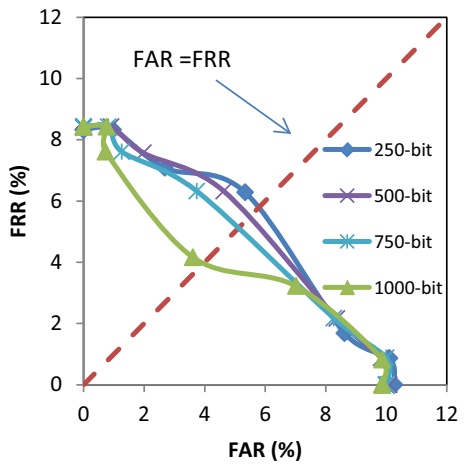

Figure 21. DET curve for different length feature vector for CASIA database.

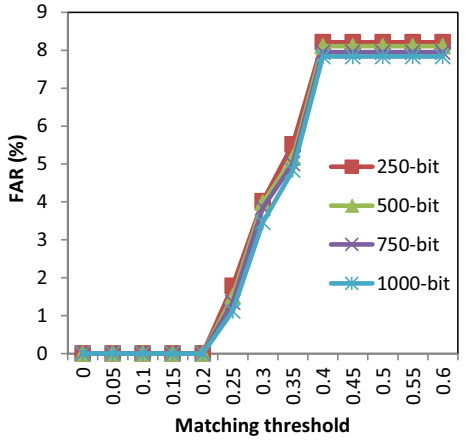

Figure 22. Variation in FAR for different length feature vector for IITD database.

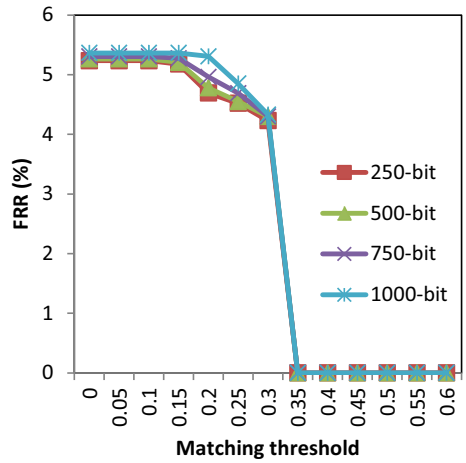

Figure 23. Variation in FRR for different length feature vector for IITD database.

threshold value of Hamming distance from 0 to 0.6 (with an increment of 0.1) decreases FRR and increases FAR of the system for both databases. The two errors become equal at threshold value of 0.31. Increasing the size of binary feature vector from 50-bit to 200-bit, FAR decreases and FRR increases at a given value of matching threshold. Figures 8 and 9 depict DET curves for IITD and CASIA databases, respectively. One can note that EER decreases with increase in feature vector size. Table 2 contains the comparison of EER for feature vectors with different sizes.

Results given in table 2 suggest that when radial resolution is increased from 50 to 200, EER decreases from 4.30% to 3.19% for IITD database and this decreases from 5.54% to 4.32% for CASIA database. As such, for a given set of statistical features, increasing radial resolution with normalization improves the performance of IRS.

Increasing number of features from three to six for experiment along concentric circles one can infer from figures 10, 11, 12 and 13 that increase in matching

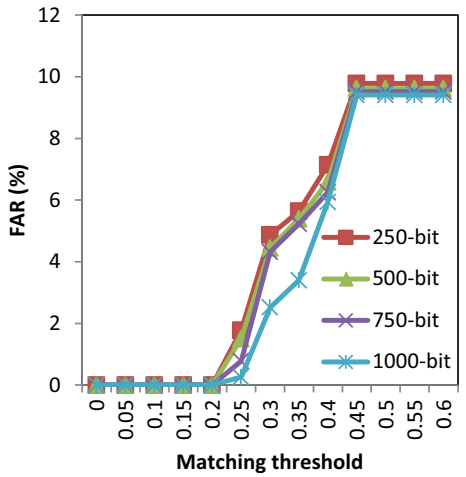

Figure 24. Variation in FAR for different length feature vector for CASIA database.

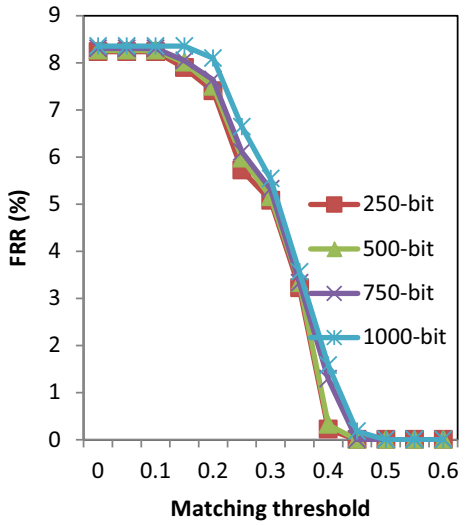

Figure 25. Variation in FRR for different length feature vector for CASIA database.

threshold from 0 to 0.6 (with an increment of 0.1) has similar effect on the variations in FAR and FRR. Using DET curves shown in figures 14 and 15 EER for two databases is computed at different radial resolutions while normalization and the same are given in table 3. When radial resolution is increased, the EER decreases from 4.25% to 1.37% for IITD database and this decreases from 5.03% to 1.55% for CASIA database.

These two experiments based on different sets of statistical features show that there is a significant improvement in FAR, FRR and EER as the number of statistical parameters for feature extraction from iris images is increased from three to six. The proposed statistical feature extraction based IRS along concentric circles is simple and effective with EER 1.37% for IITD database and 1.55% for CASIA database.

Table 2. EER for three parameters with variations in radial resolution.

Radial resolution	IIT Delhi database EER (%)	CASIA database EER (%)
50	4.30	5.54
100	3.97	5.17
150	3.70	4.87
200	3.19	4.32

Table 3. EER for six parameters with variations in radial resolution.

Radial resolution	IIT Delhi database EER (%)	CASIA database EER (%)
50	4.25	5.03
100	3.14	3.93
150	2.88	3.08
200	1.37	1.55

Table 4. EER for three parameters with variations in angular resolution.

Angular resolution	IIT Delhi database EER (%)	CASIA database EER (%)
250	4.39	5.72
500	4.22	5.42
750	4.17	5.08
1000	4.08	4.03

Second set of experiments has been conducted by extracting features along the angular direction. Initially, IRS performance has been measured by considering three parameters and later number of parameters has been increased from three to six. For three parameters, one can note from figures 16, 17, 18 and 19 that the variations in FAR and FRR of IRS is similar to the variations observed in the first experiment. Increasing the size of binary feature vector from 250-bit to 1000-bit, FAR decreases and FRR increases at a given value of matching threshold. Table 4 contains the comparison of EER for feature vector with different sizes.

Results given in table 4 suggest that if angular resolution is increased from 250-bit to 1000-bit, EER decreases from 4.39% to 4.08% for IITD database and decreases from 5.72% to 4.03% for CASIA database. As such, for a given set of statistical features, increasing angular resolution with normalization improves the performance.

It can be noted from figures 22, 23, 24 and 25 that trend of variations in FAR and FRR for six parameters along angular direction is same as depicted in earlier experiments. EER is again computed for two databases at different angular resolutions while normalization and is given in table 5.

Table 5. EER for six parameters with variations in angular resolution.

Angular resolution	IIT Delhi database EER (%)	CASIA database EER (%)
250	4.07	4.92
500	4.04	4.68
750	3.94	4.63
1000	3.66	3.44

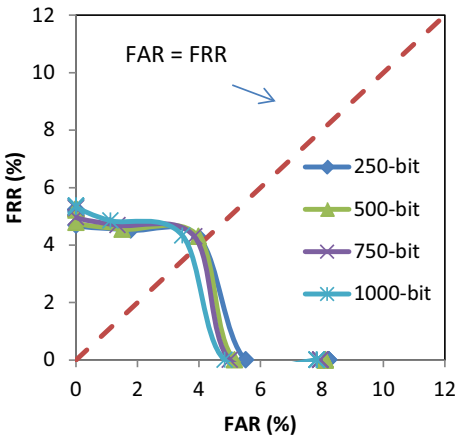

Figure 26. DET curve for different length feature vector for IITD database.

When angular resolution is increased, EER decreases from 4.07% to 3.66% for IIT Delhi database and this decreases from 4.92% to 3.44% for CASIA database as shown in figures 26 and 27.

These two experiments based on different sets of statistical features again emphasize that there is an improvement in FAR, FRR and EER, as the number of statistical parameters for feature extraction from iris images is increased from three to six. Proposed statistical feature extraction based IRS along angular direction achieves EER of 3.66% for IIT Delhi database and of 3.44% for CASIA database.

This is worth mentioning here that performance of the proposed system improves with increased number of features but the database becomes too large to handle. One can employ principal component analysis to determine significant statistical features. Increasing angular/radial resolution also improves the system performance, but at the expense of large size of feature vector set. In this work, experiments have also been conducted by taking radial resolution as 400 and angular resolution as 2000. It has been noted that the EER improves by a maximum of 0.02% when the radial resolution is taken as 400 and angular resolution as 2000 for different experiments. The accuracy of IRS might further be improved by using artificial neural network/support vector machine approach for template matching. Moment based features can also be explored for improving the

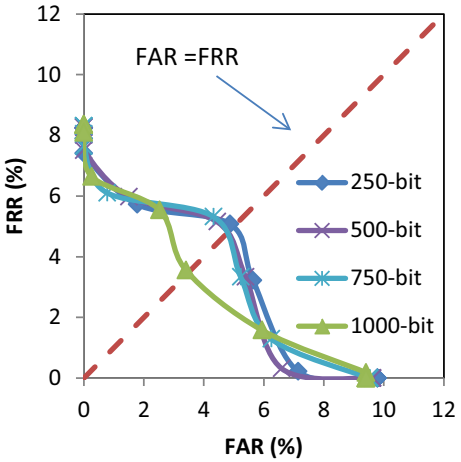

Figure 27. DET curve for different length feature vector for CASIA database.

accuracy of IRS. In our earlier work [26], Iris recognition system using statistical feature extraction technique proposed by Ko *et al* [6] and Kyaw [7] were implemented in the same environment. We also implemented 1-D log-Gabor wavelet filter method [27] for feature extraction in the same environment.

In the proposed technique the length of iris code (number of bits) is *number of features* × *radial resolution* in case of feature extraction along concentric circles and it is *number of features* × *angular resolution* in case of feature extraction along the angular direction. Therefore, maximum length of iris code obtained for experiment along radial direction is $6 \times 200 = 1200$ bits and that along angular direction is $6 \times 1000 = 6000$ bits. While the length of iris code in case of 1-D log-Gabor wavelet filter technique is 2 × *radial resolution* × *angular resolution* [27]. So even the normalized iris pattern of size 20 × 240. would produce iris code of length 9600 bits. Therefore, the proposed approach creates a compact 150-byte (radial direction) or 750-byte (angular direction) size template as compared to 1200-byte size template in case of 1-D log-Gabor wavelet filter technique, which allows for efficient storage and comparison of irises.

Table 6 contains the comparison of proposed approach with these algorithms in terms of most effective EER, iris code length and iris code creation time. Experiments with different feature extraction algorithms have been carried out in the same computing environment. Table 6 shows that the performance of proposed iris recognition system based on statistical feature extraction technique is comparable, effective and encouraging. Here, it is worth mentioning that the proposed statistical feature extraction based iris recognition creates a compact iris code, requires less memory to store the database and takes less time to compute iris code as compared to other mentioned techniques.

Table 6. Comparison of proposed approach with existing techniques.

Feature extraction technique	IIT Delhi database EER (%)	CASIA database EER (%)	Iris code length (bits)	Iris code creation time (ms)
Statistical without normalization	19.30	22.00	120	210
Cumulative sum based change analysis	1.50	2.70	320	204
1-D log-Gabor wavelet	1.27	1.50	9600	204
Proposed approach (angular direction)	3.66	3.44	6000	178
Proposed approach (radial direction)	1.37	1.55	1200	134

7. Conclusion

A statistical feature extraction based IRS has been proposed and implemented in this work. It is demonstrated that statistical features can be computed along radial and angular directions. System performance in both the directions is satisfactory. Experimental results obtained for IRS based on statistical feature extraction technique are encouraging. It has been seen that system performance is improved with increased number of statistical features. Results also show that increased radial or angular resolution while normalization in place improves the accuracy of IRS. Experimentation with varying angular and radial resolution suggests that 200-bit feature vector for statistical feature extracted along radial direction while 1000-bit feature vector for statistical feature extraction along angular direction gives a good performance of IRS. Comparison between test image template and templates stored in the database is carried out using Hamming distance. The most effective error rate achieved in the experiments conducted in this work is 1.37% when 200-bit feature vector along radial direction is considered and is 3.44% when 1000-bit feature vector along angular direction is considered. Results also show that statistical feature extraction based technique creates compact iris code and takes less time for feature extraction.

References

[1] Giot R, Hemery B and Rosenberger C 2010 Low cost and usable multimodal biometric system based on keystroke dynamics and 2-*D* face recognition. In: *Proceedings of twentieth IEEE international conference on pattern recognition*, 23–26 August 2010, pp. 1128–1131

[2] Cao K, Eryun L and Jain A K 2014 Segmentation and enhancement of latent fingerprints: A coarse to fine ridge structure dictionary. *IEEE Trans. Pattern Anal. Mach. Intell.* 36(9): 1847–1859

[3] Senoussaoui M, Kenny P, Stafylakis T and Dumouchel P 2014 a study of the cosine distance-based mean shift for telephone speech diarization. *IEEE Trans. Audio, Speech Language Process.* 22(1): 217–227

[4] Daugman J 1993 High confidence visual recognition of persons by a test of statistical independence. *IEEE Trans. Pattern Anal. Mach. Intell.* 15: 1148–1161

[5] Daugman J 2004 How iris recognition works? *IEEE Trans. Circuits Syst. Video Technol.* 14(1): 21–30

[6] Ko Jong Gook, Gil Yeon Hee and Yoo Jang Hee 2006 Iris recognition using cumulative sum based change analyses. *International symposium on intelligent signal processing and communication system,* pp. 275–278

[7] Kyaw Khin Sint Sint 2009 Iris recognition system using statistical features for biometric identification. In: *Proceedings of international conference on electronic computer technology.* pp. 554–556

[8] Bansal A, Agarwal R and Sharma R K 2010 Trends in iris recognition algorithm. In: *Proceedings of IEEE Fourth Asia international conference on mathematical/analytical modeling and computer simulation,* pp. 337–340

[9] He Zhaofeng, Tan Tieniu, Sun Zhenan and Qiu Xianchao 2009 Toward accurate and fast iris segmentation for iris biometrics. *IEEE Trans. Pattern Anal.Mach. Intell.* pp. 1670–1684

[10] Kumar A and Passi A 2010 Comparison and combination of iris matchers for reliable personal authentication. *Pattern Recognit.* 43(3): 1016–1026

[11] Li Su, Qian Li and Xin Yuan 2011 Study on algorithm of eyelash occlusions detection based on endpoint identification. In: *Proceedings of third international workshop on intelligent systems and applications (ISA),* pp. 1–4

[12] Bodade R M and Talbar S N 2009 Shift invariant iris feature extraction using rotated complex wavelet and complex wavelet for iris recognition system. *Proceeding of seventh international conference on advances in pattern recognition*, pp. 449–452

[13] Tisse C, Martin L, Torres L and Robert M 2002 Person identification technique using human iris recognition. In: *Proceedings of international conference on vision interface,* Canada. pp. 294–299.

[14] Tsai Chung Chih, Lin Heng Yi, Taur Jinshiuh and Tao Ching Wang 2012 Iris recognition using possibilistic Fuzzy matching on local features. *IEEE Trans. Syst. Man Cybern. – B: Cybern.* 42(1): 150–162

[15] Vivek S A, Aravinth J and Valarmathy S 2012 Feature extraction for multimodal biometric and study of fusion using Gaussian mixture model. In: *Proceedings of the*

international conference on pattern recognition, informatics and medical engineering. pp. 387–392

[16] Sundaram R M and Dhara B C 2011 Neural network based iris recognition system using Haralick features. In: *Proceeding of IEEE third international conference on electronics computer technology* pp. 19–23

[17] He Y, Feng G, Hou Y, Li L and Tzanakou E M 2011 Iris feature extraction method based on LBP and chunked encoding, *IEEE seventh international conference on natural computation,* pp. 1663–1667

[18] Rahulkar A D and Holambe R S 2012 Half-Iris feature extraction and recognition using a new class of biorthogonal triplet half-band filter bank and flexible k-out-of-n: A post classifier, *IEEE Trans. Information Forensics Security.* 7(1): 230–240

[19] Costa R M D and Gonzaga A 2012 Dynamic features for iris recognition. *IEEE Trans. Syst. Man Cybern. – B: Cybern.* 42(4): 1072–1082

[20] Ballard D H 1981 Generalizing the Hough transform to detect arbitrary shapes. *Pattern Recognit.* 13(2): 111–122

[21] Wildes R, Asmuth J, Green G, Hsu S, Kolczynski R, Matey J and McBride S 1994 A system for automated iris recognition. In: *Proceedings of IEEE workshop on applications of computer vision.* pp. 121–128

[22] Kong W and Zhang D 2001 Accurate iris segmentation based on novel reflection and eyelash detection model. In: *Proceedings of international symposium on intelligent multimedia, video and speech processing.* pp. 263–266

[23] Ma L, Wang Y and Tan T 2002 Iris recognition using circular symmetric filters. *National Laboratory of Pattern Recognition, Institute of Automation, Chinese Academy of Sciences.* pp. 414–417

[24] Zhu Yong, Tan Tieniu and Wang Yunhong 2000 Biometric personal identification based on iris patterns. In: *Proceedings of the IEEE international conference on pattern recognition.* pp. 2801–2804

[25] Huang J, Wang Y, Tan T and Cui J 2004 A new iris segmentation method for recognition. In: *Proceedings of the seventeenth international conference on pattern recognition,* vol. 3 pp. 554–557

[26] Bansal A, Agarwal R and Sharma R K 2012 FAR and FRR based analysis of iris recognition system. *IEEE international conference on signal processing, computing and control (ISPCC'12),* pp. 1–6

[27] Masek L 2003 *Recognition of human iris patterns for biometric identification. Technical report*, School of Computer Science and Software Engineering, University of Western Australia